Acta Crystallographica Section D
Biological Crystallography
ISSN 0907-4449

The role of protein and surfactant interactions in membrane-protein crystallization

Bryan W. Berger,[a] Colleen M. Gendron,[a] Clifford R. Robinson,[b] Eric W. Kaler[a] and Abraham M. Lenhoff[a]*

[a]Center for Molecular and Engineering Thermodynamics, Department of Chemical Engineering, University of Delaware, Newark, DE 19716, USA, and [b]Delaware Biotechnology Institute and Department of Chemistry and Biochemistry, University of Delaware, Newark, DE 19716, USA

Correspondence e-mail: lenhoff@che.udel.edu

Received 17 July 2004
Accepted 9 November 2004

The interactions leading to crystallization of the integral membrane protein bacteriorhodopsin solubilized in *n*-octyl-β-D-glucoside were investigated. Osmotic second virial coefficients were measured by self-interaction chromatography in the presence of sodium malonate, sodium formate and ammonium sulfate. Attractive protein–detergent complex (PDC) interactions were observed as the surfactant cloud-point temperature was approached for each salt, suggesting that surfactant interactions may play an important role in promoting PDC crystallization. Dynamic light scattering and tensiometry measurements show that the interaction trends are strongly influenced by micelle structure and surfactant phase behavior, both of which are sensitive to salt and surfactant concentration. Overall, detailed investigations using a combination of experimental techniques can provide insight into the complex nature of PDC interactions, which is essential to developing rational approaches to membrane-protein crystallization.

1. Introduction

Despite the importance of membrane proteins in biological processes such as signal transduction as well as their potential as targets for therapeutic agents, there remains a significant lag in obtaining structural information for these proteins relative to water-soluble proteins. A primary reason for this lack of information is the inherent insolubility of membrane proteins in aqueous solutions. In many cases, more than half the surface of the integral membrane protein is buried within the membrane, the hydrophobic environment of which is considerably different to that of the extracellular or cytoplasmic space (von Heijne, 1994). Surfactants have played an essential role in overcoming this difficulty to prepare soluble samples for further study. Solubilization of membrane proteins is typically achieved through use of non-ionic surfactants at concentrations greater than their respective critical micelle concentrations (CMC), where the hydrocarbon tail of the surfactant preferentially associates with the transmembrane portions of the protein to displace the membrane and form a soluble protein–detergent complex (PDC) (Garavito *et al.*, 1996). As such, PDCs form a basis for subsequent characterization or crystallization.

Previous work has suggested that the likelihood of membrane protein crystallization from a PDC may be enhanced under conditions near a surfactant cloud point temperature (Garavito *et al.*, 1986). The cloud point temperature, which is a lower consolute temperature, is a feature of many non-ionic surfactant systems at which separation into two equilibrium liquid phases occurs. Attractive surfactant–surfactant interactions are expected to be significant near this phase transition, and therefore to participate constructively in PDC crystallization under such conditions. In particular, previous studies with Outer Membrane Protein F (OmpF) from *E. coli* using either *n*-octyl-β-D-glucoside ($C_8\beta G_1$) or octyl–polyoxyethylene (octyl–POE) in combination with precipitants such as sodium chloride and polyethylene glycol (PEG) were performed at conditions near cloud point temperatures (Garavito & Rosenbusch, 1986). However, the effects of either sodium chloride or PEG on the interactions between the various components leading to crystallization remain unclear.

The use of the surfactant cloud point temperature as a guide to obtaining membrane protein crystals provides an approach to protein crystallization based on solution properties rather than empirical screens. For soluble proteins, such approaches have focused heretofore largely on the relationship between the osmotic second virial coefficient (B_{22}) of a protein and solution conditions leading to crystallization. B_{22} is a dilute solution property that reflects net, pairwise protein interactions in solution (McQuarrie, 2000),

$$B_{22} = -\frac{1}{2}\int_0^\infty \int_{\Omega_1} \int_{\Omega_2} [\exp(-W/kT) - 1]\, dr_{12}\, d\Omega_1\, d\Omega_2,$$

where k is Boltzmann's constant and T is temperature. W is the potential of mean force and reflects the pairwise interactions between protein molecules 1 and 2 in solution as a function of separation distance r_{12} and orientations Ω_1 and Ω_2. A pioneering study of several soluble proteins suggested that solution conditions that produce protein crystals are generally those corresponding to slightly negative values of B_{22} (George & Wilson, 1994). This led to the concept of the crystallization slot as a range of B_{22} values from -0.8 to -8 mol ml g^{-2} to guide selection of solution conditions that may promote crystal growth. Recently, this characterization was extended to PDCs involving OmpF and mixed micelles of $C_8\beta G_1$ and octyl–POE (Hitscherich *et al.*, 2000), where B_{22} values for PDC solutions at conditions known previously to produce diffraction-quality crystals were shown to correspond to values within or near the crystallization slot. Interestingly, similarly attractive B_{22} values were also obtained for corresponding micelle solutions, suggesting that the surfactant not only may play a constructive role in PDC crystallization, but that aspects of its phase behavior could also be used as an indicator of conditions favorable for crystallization (Loll *et al.*, 2001, 2002).

Traditional methods of determining B_{22} such as static light scattering (SLS) can be difficult to extend to PDCs, where the effects of aggregation and multiple species make measurement of B_{22} challenging. This is a particular problem for membrane proteins, which are often crystallized from mixtures of PDCs and free micelles, the structures of which can change significantly with solution conditions. Therefore, self-interaction chromatography (SIC) has become a valuable technique for studying both soluble and membrane protein crystallization. SIC is a recently developed method in which the protein of interest is covalently attached to chromatographic particles and packed into a column. The relative retention of the same protein in the mobile phase is then measured as a function of solution conditions (Patro & Przybycien, 1996). If the protein is immobilized in sufficiently random fashion, one can relate the chromatographic retention to B_{22} without the use of adjustable parameters, allowing for a quantitative assessment of interactions at various solution conditions (Tessier, Lenhoff *et al.*, 2002). For several water-soluble proteins, B_{22} values measured by SIC are in quantitative agreement with those obtained from SLS and neutron scattering, demonstrating that SIC can provide a rapid, effective means of determining B_{22} (Tessier *et al.*, 2003; Tessier, Vandrey *et al.*, 2002).

Here, we present osmotic second virial coefficients as determined by self-interaction chromatography for bacteriorhodopsin–$C_8\beta G_1$ PDCs. These results are interpreted in terms of the corresponding surfactant phase behavior and protein characteristics as a function of solution conditions in order to understand the roles that each may play in promoting PDC crystallization.

2. Materials and methods

2.1. Materials

1-Ethyl-3-(3-dimethylaminopropyl)carbodiimide (EDC; 22980), *N*-hydroxysuccinimide (NHS; 24500) and the Micro BCA Protein Assay Kit (23231, 23232, 23234) were obtained from Pierce. *n*-Octyl-β-D-glucoside ($C_8\beta G_1$; O311) was from Anatrace. 2-(*N*-Morpholino)-ethanesulfonic acid (MES; M8250), sodium malonate (M4795), sodium formate (F4166), ammonium sulfate (A4915) and cell culture reagents were from Sigma. AF-Amino-650M particles (08002) were from Tosoh Biosep. 3 mm × 50 mm borosilicate glass microcolumns (993301) were from P. J. Cobert and Associates.

2.2. Procedures and analysis

2.2.1. Expression and purification of BR. BR was expressed and purified from Vac$^-$ Rub$^-$ *Halobacterium halobium* strain ET1001, which constitutively overexpresses BR, as described previously (DasSarma & Fleischmann, 1995; Shand & Betlach, 1994). Purple membrane (PM) concentration was determined by measuring the absorbance at 550 nm using an extinction coefficient of 58 000 M^{-1} cm^{-1} (Miercke *et al.*, 1988); typical yields were 15–20 mg of purple membrane per litre of cell culture with a 280 to 550 nm absorbance ratio of 1.8 or less. For solubilization, PM was diluted to 0.5 mg ml^{-1} in 10 m*M* MES buffer pH 6.5 and 100 m*M* $C_8\beta G_1$ was added. The solution was allowed to stand for 48 h, after which residual PM was removed by centrifugation for 1 h at 100 000*g*. The PDC solution was then concentrated using an Amicon Ultra 30 000 or 50 000 MWCO centrifugal filter. BR concentration was determined by measuring the absorbance at 568 nm using an extinction coefficient of 63 000 M^{-1} cm^{-1} (Dencher & Heyn, 1978). Purity and homogeneity were checked using dynamic light scattering and SDS–PAGE.

2.2.2. Self-interaction chromatography. Preparation of immobilized BR particles for self-interaction chromatography and subsequent measurements were performed using a procedure modified from that reported previously (Tessier, Vandrey *et al.*, 2002). BR was immobilized on AF-Amino-650M particles by using EDC and NHS to attach BR covalently *via* its surface-accessible carboxylic acid groups to the primary amine groups on the particle surface (Sehgal & Vijay, 1994). 0.5 ml of settled particles were washed extensively with water and resuspended in 7 ml of 20 m*M* MES pH 6 buffer containing 70 m*M* $C_8\beta G_1$. This was allowed to mix for 1 h, after which time a PDC solution at a BR concentration of 3–6 mg ml^{-1} was added. Approximately 2 mg NHS and 60 mg EDC were then added and the solution allowed to mix at room temperature in the dark for 8 h. This solution was then washed with 20 m*M* MES pH 6 buffer containing 70 m*M* $C_8\beta G_1$. Samples were collected from each wash and the particles stored at 4°C. Immobilized protein concentrations were determined by a mass balance based on the residual protein in the wash solutions using values based on visible absorbance at 568 nm as well as from a direct measurement of the particles using a membrane protein compatible micro BCA method as per manufacturer's instructions. Typical immobilization densities were 10–15 mg of BR per ml of settled particles, corresponding to roughly 15% surface coverage. Packing into a 0.35 ml borosilicate glass microcolumn, calibration and sample runs were essentially as described previously (Tessier, Lenhoff *et al.*, 2002), except that 20 column volumes were typically required to pre-equilibrate the column at a given solution condition. Also, all wash steps after elution were made for five column volumes at low salt concentration to prevent aggregation. In all cases, SIC measurements were made in the dark at 23 ± 2°C using

10 m*M* MES buffer pH 6.5 with $C_8\beta G_1$ present at concentrations above the CMC.

Chromatographic retention is typically characterized in terms of the retention factor k' (Guiochon *et al.*, 1994),

$$k' = \frac{V_r - V_o}{V_o}.$$

Here V_r refers to the retention volume of the solute as it passes through the column at a given solution condition of interest and V_o refers to the retention volume at a solution condition where the solute does not interact with the particle surface. Not unexpectedly, increasing salt concentration led to aggregation, especially near the surfactant phase boundary. However, at lower surfactant concentrations aggregation was significantly reduced. Furthermore, appearance of aggregate coincided with increasing peak asymmetry. Thus, acceptable values of V_r were limited to solution conditions where the final PDC concentration was within the range where no injection concentration dependence and peak asymmetry were observed. Estimates of V_o were made using 1%(*v*/*v*) acetone and corrected for differences in effective pore volume due to immobilized protein as described previously (Tessier, Lenhoff *et al.*, 2002).

B_{22} is calculated according to the relation (Tessier, Lenhoff *et al.*, 2002)

$$B_{22} = B_{22}^{HS} - \frac{k'}{\rho_s \varphi}$$

where ρ_s refers to the immobilization density, or the amount of protein immobilized per unit accessible surface area of the pore, which can be calculated as described above. The phase ratio φ represents the total accessible surface area of the pore space per unit volume of settled particles and is a property of the chromatographic material used (DePhillips & Lenhoff, 2000); in this case, the presence of immobilized protein is taken into consideration as well in determining accessibility. Due to the varying nature of the surfactant structure as a function of solution conditions, PDC radii were determined using dynamic light scattering. These were found to remain relatively constant until solution conditions near the cloud point of the surfactant were reached. Therefore, average values of PDC radii determined from DLS were used to calculate the hard sphere contribution B_{22}^{HS}, which are in good agreement with molecular volumes of a BR–$C_8\beta G_1$ PDC determined by dynamic relaxation NMR as well as from crystallographic data (Connolly, 1983; Gottschalk *et al.*, 2001).

2.2.3. Cloud point temperature measurements. 1 ml samples were prepared in pre-cleaned glass vials at a given pH, precipitant and additive concentration from corresponding stock solutions and allowed to equilibrate at 25°C for 1 h in a Braun Thermomixer water bath with temperature control to 0.1°C; independent temperature measurements were made using an Omega HH21 thermocouple. The onset of clouding was determined by visual inspection and was defined as the lowest temperature at which the solution spontaneously became turbid. This method has been successfully applied to determining the phase behavior of a wide variety of non-ionic and zwitterionic surfactants (Balzer, 1996; Blankschtein *et al.*, 1986; Liu *et al.*, 1996). In all cases, the 'clouding' transition was sharp and occurred instantly, justifying use of the macroscopically observed clouding as an accurate measure of the cloud point temperature (Laughlin, 1994). Initially, the sample temperature was increased in 1–5°C increments and equilibrated for 5 min to locate an approximate phase boundary. The experiment was then repeated, increasing temperature in 0.1°C increments and equilibrating for at least 15 min. The temperature was then raised and lowered repeatedly to ensure reproducibility of each cloud point temperature measurement (Blankschtein *et al.*, 1986).

2.2.4. Dynamic light scattering (DLS). DLS measurements were made using a Brookhaven instrument with a BI200SM goniometer and BI9000AT digital correlator. The light source was a Lexel 488 nm Ar laser operated at 100 mW. The hydrodynamic radius R_H was obtained from the diffusion coefficient D using the Stokes–Einstein relation. Solutions were allowed to incubate for 12 h in the dark at a given temperature prior to analysis. All measurements were made at 20°C using 10 m*M* MES pH 6.5 buffer.

2.2.5. Tensiometry. The surface tensions of surfactant solutions containing salts or additives were measured by the Wilhelmy plate method using a Kruss tensiometer. All measurements were made at 20°C using 10 m*M* MES pH 6.5 buffer. Measurements at a given precipitant, additive and surfactant concentration were repeated in triplicate to ensure reproducibility. The CMC was determined from the breakpoint in a plot of surface tension *versus* log concentration at a given solution condition. Samples were allowed to equilibrate for 1 h after dilution.

2.2.6. Crystallization. Crystallization of BR was performed using a microbatch method. In microbatch, 2 µl of a 5–10 mg ml^{-1} PDC solution at pH 6.5 and intermediate precipitant concentration far from the onset of attractive B_{22} values or significant aggregation was added to 2 µl of either buffer or concentrated additive solution and mixed briefly. To this, 2 µl of concentrated precipitant solution was added, thereby diluting to desired concentrations of all components. Conventional hanging drops for crystallization were prepared against reservoirs containing the same precipitant and additive concentrations. Crystals appeared within four weeks as determined by optical microscopy, whereas precipitation and surfactant phase separation could often be observed within days.

3. Results

3.1. Effect of salt type and concentration

Bacteriorhodopsin has been crystallized in multiple forms from $C_8\beta G_1$ PDCs using high concentrations of ammonium sulfate or potassium phosphate in a range of pH values from 4–6 (Landau & Rosenbusch, 1996; Luecke *et al.*, 1999; Sato *et al.*, 1999; Schertler *et al.*, 1993, 1991; Takeda *et al.*, 1998). BR has an experimentally determined isoelectric point of 5.5 (Miercke *et al.*, 1989). In most cases, the authors observed significant precipitation and surfactant phase separation along with crystal formation, limiting the overall crystal quality. With this in mind, ammonium sulfate was chosen as a basis of comparison along with sodium malonate and sodium formate. The motivation for using malonate and formate comes from a recent crystallization screen for soluble proteins in which the frequency of success using malonate and formate was higher in most cases than for the more commonly used ammonium sulfate (McPherson, 2001).

The effect of solution conditions on interactions involving PDCs and $C_8\beta G_1$ was investigated by measuring B_{22} values for the $C_8\beta G_1$–BR PDC (Fig. 1*a*) and $C_8\beta G_1$ cloud point temperatures (Fig. 1*b*). At low to moderate salt concentrations, the PDC B_{22} values show an increase in repulsive interactions, followed by a sharp transition to attractive PDC interactions in a narrow range of high salt concentrations. Interestingly, the sharp crossover to attractive interactions coincides with the respective $C_8\beta G_1$ cloud curves, the steepness of which is similar to that of the attractive regions of the corresponding B_{22} plots for the PDC. This suggests that for a PDC solution at a fixed surfactant concentration above its CMC, the surfactant interactions may play a significant role in determining the onset of attractive PDC

interactions. The sensitivity of both the PDC interactions and $C_8\beta G_1$ cloud point temperature to salt concentration also limits the possible solution conditions that fall within the weakly attractive crystallization slot.

In order to understand the nature of these surfactant effects on PDC interactions, the microstructure and phase behavior were examined in greater detail using dynamic light scattering (DLS) and surface tension measurements. Over the range of salt concentrations used in crystallization, the CMC of $C_8\beta G_1$ decreases by at least an order of magnitude, as shown in Fig. 2; similar results have been observed previously for $C_8\beta G_1$ as well in the presence of high ammonium sulfate concentrations (Lorber *et al.*, 1991). DLS results in Fig. 3 show that the nominal apparent diameter of 5.2 nm for the micelle at 40 m*M* $C_8\beta G_1$ grows to over 50 nm at ionic strengths above 2 *M*. It is important to note that this is only an estimate of apparent radius, as the interactions between components and deviations from sphericity preclude accurate determination of size, particularly near the cloud point temperature at which attractive interactions, and therefore larger apparent sizes, are expected to be significant. However, these results are consistent with previous quantitative characterization of $C_8\beta G_1$ micelle structure by small-angle X-ray and neutron scattering, in which the trend of increased size is observed at high salt concentrations (Thiyagarajan & Tiede, 1994; Zhang *et al.*, 1999).

3.2. Effect of surfactant concentration

It has been suggested that surfactant concentrations in a range of 2–10 × CMC are effective in solubilizing and crystallizing membrane proteins (Hunte, 2002). However, as mentioned above, the CMC and surfactant phase behavior are highly sensitive to solution conditions common to membrane protein crystallization. Therefore, the effect of lowering surfactant concentration after extraction was examined, particularly in relation to the CMC value at a given salt concentration. Concentrations less than 2 × CMC led to substantial aggregation and inactivation at high salt concentrations such that B_{22} values could not be reliably measured; this may represent a limiting case for the amount of surfactant necessary to solubilize BR adequately at a concentration of 1 mg ml^{-1}. However, as shown in Fig. 4, simultaneously varying the $C_8\beta G_1$ and salt concentration so as to remain at 2 × CMC for all samples leads to a significant decrease in the apparent PDC repulsion, especially at low to moderate ionic strengths. Furthermore, a more gradual transition to attractive PDC interactions is observed, giving rise to a wider range of solution concentrations corresponding to weakly attractive PDC interactions.

Reducing the surfactant concentration also changes the cloud point temperature at a given solution condition. Fig. 5 shows that at 20 m*M* $C_8\beta G_1$, which is the lowest concentration used in this study, the cloud point temperature is 15–20°C above that at 40 m*M* $C_8\beta G_1$, which was used initially. Thus, in general the attractive PDC interactions observed still coincide with the appearance of a surfactant phase boundary, although their interactions are diminished. DLS results in Fig. 6 reveal that the apparent size of the micelles increased by less than a factor of two at 2 × CMC over the range of salt concentrations used for crystallization, whereas at a fixed concentration of 40 m*M* $C_8\beta G_1$ the apparent diameter increased by over an

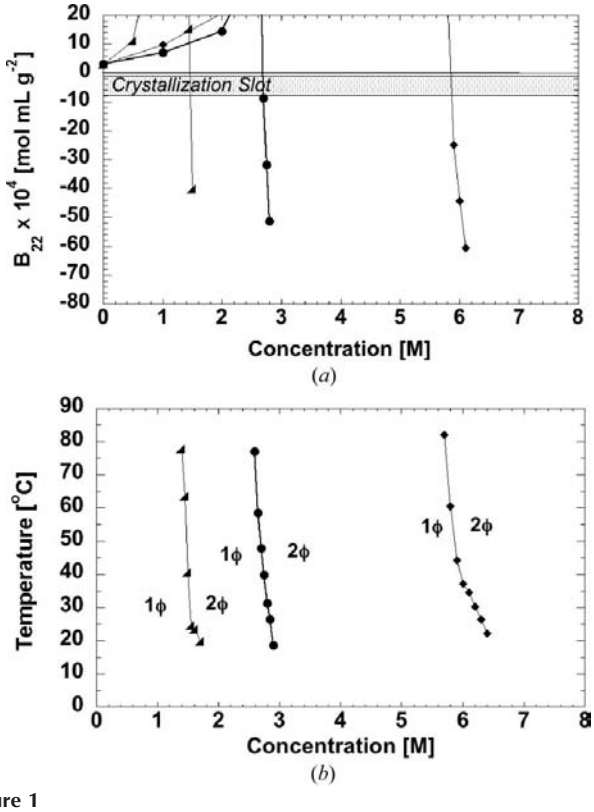

Figure 1
Effect of salt type and concentration on bacteriorhodopsin PDC B_{22} values (*a*) and $C_8\beta G_1$ cloud point temperatures (*b*) for ammonium sulfate (circles), sodium malonate (triangles) and sodium formate (diamonds). The $C_8\beta G_1$ concentration is 40 m*M* in all cases.

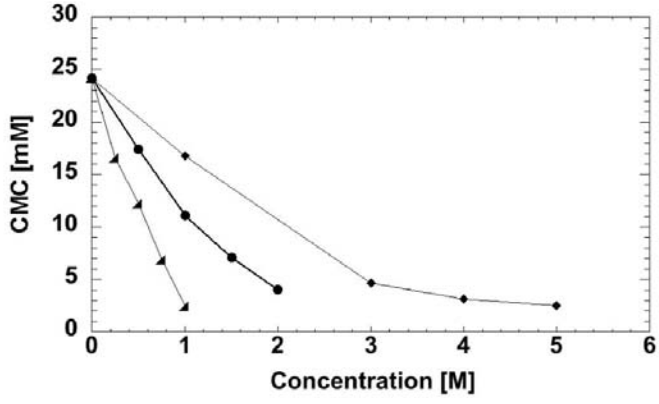

Figure 2
Decrease in CMC for $C_8\beta G_1$ with increasing salt concentration for ammonium sulfate (circles), sodium malonate (triangles) and sodium formate (diamonds).

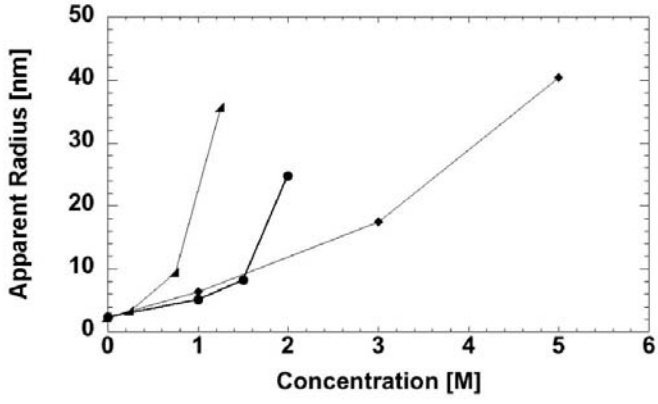

Figure 3
Apparent hydrodynamic radius of micelles at 40 m*M* $C_8\beta G_1$ with increasing concentration of ammonium sulfate (circles), sodium malonate (triangles) and sodium formate (diamonds) as determined by DLS.

order of magnitude. Therefore, reducing surfactant concentration leads to a higher cloud point temperature and reduced attractive surfactant interactions as well as reduced apparent micelle size.

4. Discussion

4.1. Relationship between surfactant phase behavior and PDC interactions

Precipitants such as ammonium sulfate are often thought to influence primarily protein–protein interactions during crystallization, whereas the surfactant is assumed to play mainly a passive role in solubilizing the membrane protein. However, the results here confirm previous observations in demonstrating that the surfactant also has a major influence on PDC interactions (Hitscherich *et al.*, 2000; Loll *et al.*, 2001). Our investigation of the underlying phenomena provides further insight into these effects based on the precipitants used, but general patterns of PDC interactions can be identified as a consequence of differences in surfactant phase behavior. Specifically, the substantial reduction in CMC with increasing salt concentration for micelle solutions, along with the increase in apparent micelle size observed by light scattering, suggest that with increasing ionic strength, the distribution of micelle sizes changes, favoring larger, non-spherical shapes. This, in turn, may preclude the PDCs from interacting productively and would explain the substantial repulsion with increasing ionic strength observed for ammonium sulfate, sodium malonate and sodium formate. In this case, the attraction experienced as the $C_8\beta G_1$ cloud curve is approached may be masked by excluded volume interactions due to the extended micelle structure. This leads to an initial increase in the virial coefficient values, followed by a sharp decrease once the solution conditions are sufficiently close to the phase boundary to overcome this repulsion. One way of controlling this behavior is by reducing the surfactant concentration, thereby raising the $C_8\beta G_1$ cloud point temperature and reducing the attractive surfactant interactions. A practical result of this reduction in concentration is that the apparent micelle size decreases, which allows PDC–PDC interactions to occur to a greater degree. This is reflected in the B_{22} measurements, where the apparent repulsion at moderate ionic strengths is greatly reduced, leading to a wider range of weakly attractive B_{22} values.

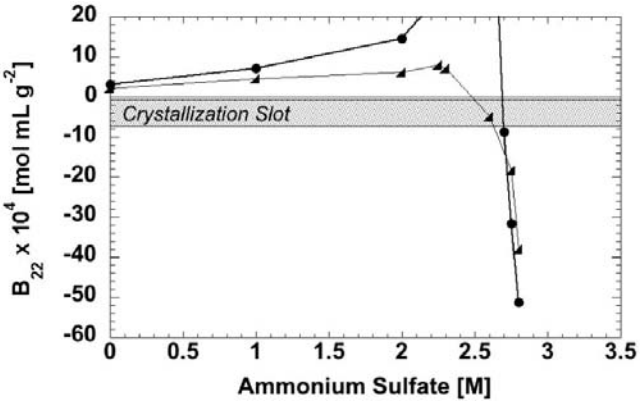

Figure 4
Effect of reduced surfactant concentration on B_{22} values for BR PDCs. Data from 40 m*M* $C_8\beta G_1$ (circles) are included for comparison; 2 × CMC (triangles) values can be determined from Fig. 2.

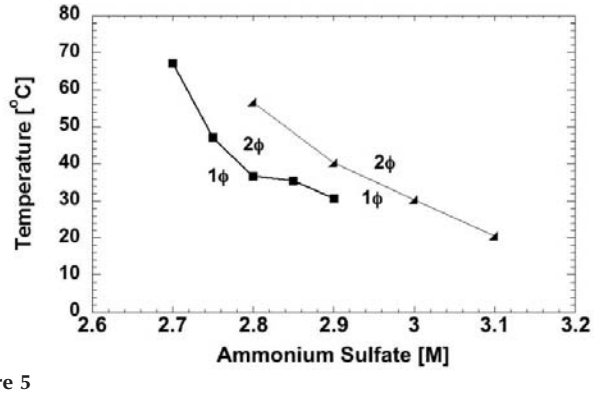

Figure 5
Effect of reducing $C_8\beta G_1$ concentration from 40 m*M* (squares) to 20 m*M* (triangles) on the cloud point temperature over the range of concentrations corresponding to attractive PDC B_{22} values.

4.2. Correlation between the cloud point and B_{22}

It is apparent from the discussion above that surfactant phase behavior and interactions play a significant role in promoting PDC crystallization. One consequence of this is the importance of micelle shape and structure in affecting PDC interactions. However, another important point is that for the various combinations of additives and precipitants studied, attractive PDC interactions tend to occur at conditions approaching the $C_8\beta G_1$ cloud curve. This was observed previously in a few specific cases for Outer Membrane Protein F, where attractive B_{22} values occurred at high PEG concentrations near the octyl–POE cloud curve (Hitscherich *et al.*, 2000). Furthermore, attractive B_{22} values for the corresponding micelle solutions followed a similar trend to that of the PDCs, again suggesting that the surfactant may play a constructive role in PDC crystallization. In order to test this hypothesis quantitatively for the present study, 30 measured osmotic second virial coefficient values for the PDC were chosen over a wide range of solution conditions for which a corresponding $C_8\beta G_1$ cloud point temperature was measured. The results were compared in terms of the dimensionless quantities:

$$T_r = \frac{T_{cloud} - T}{T_{cloud}}, \qquad B' = \frac{B_{22}}{B_{22}^{HS}}.$$

T in this case is 20 °C and refers to the temperature at which the interaction measurements and crystallization trials were performed. As shown in Fig. 7, a strong correlation exists between the measured B_{22} value of the BR–$C_8\beta G_1$ PDCs and the corresponding cloud point temperature of $C_8\beta G_1$. This clearly demonstrates the significance of $C_8\beta G_1$ for the overall process of PDC crystallization. Furthermore,

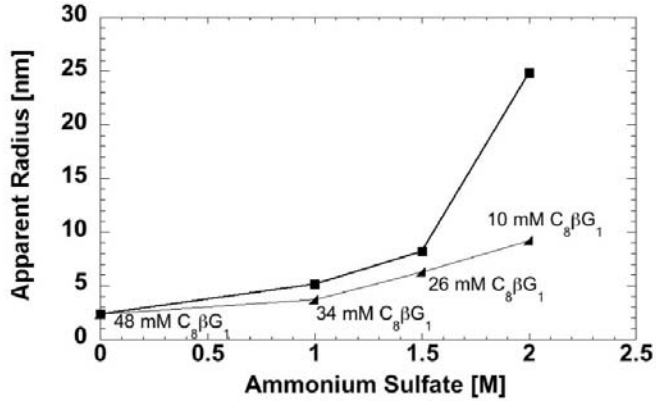

Figure 6
Effect of reducing $C_8\beta G_1$ concentration from 40 m*M* (squares) on apparent micelle size as determined by DLS. 2 × CMC (triangles) concentrations for $C_8\beta G_1$ are given for comparison at each respective ammonium sulfate concentration.

Table 1
PDC and surfactant properties of solutions that led to crystal formation.

All experiments were performed at 20°C.

Salt (*M*)	$C_8\beta G_1$ (m*M*)	$B_{22} \times 10^4$ (mol ml g^{-2})	Cloud point temperature (°C)
Ammonium sulfate			
2.65	8	−4.84	60.8
2.7	8	−10.20	54.5
2.7	40	−8.77	47.8
Sodium malonate			
1.5	6	−1.85	50.5
1.55	6	−14.64	29.4
1.6	6	−20.11	22.2
Sodium formate			
5.8	20	−4.14	54.5
5.9	5	−9.55	48.4
6	5	−18.96	42.5

crystallization trials led to crystals in a subset of these conditions, also indicated in Fig. 7 and summarized in Table 1, although in these cases precipitation was also observed. In the context of the crystallization slot, crystallization generally occurred for slightly negative values of B_{22}, consistent with the concept of weakly attractive interactions predominating under conditions favorable for crystallization. In general, these conditions fall in a range of approximately 20–30°C below the $C_8\beta G_1$ cloud point temperature. The observed scatter at lower T_r may be a result of changes in the amount of surfactant bound to the PDC in the vicinity of the cloud point temperature, which in turn affects the diameter and molecular weight used in estimation of the hard-sphere contribution to B_{22}. This trend is consistent with the ordering observed for colloidal particles suspended in a structured surfactant solution near a phase boundary. Studies of silica and other charged particles, which are functionally similar to PDCs, in non-ionic surfactant solutions demonstrated that by varying the degree of attraction between the surfactant aggregates, or proximity to the cloud point temperature, a crystalline region near the liquid–liquid phase boundary was observed (Koehler & Kaler, 1997). In these cases, the most important factor was particle shape, whereas charge density and concentration did not affect the range of interactions. Thus, the surfactant interactions driving phase separation were necessary to overcome the electrostatic repulsion between these particles, which may explain why temperatures within 1°C of the cloud point were necessary to observe crystallization. For bacteriorhodopsin, the SIC measurements were made at pH 6.5, which is within one unit of the isoelectric point. BR is also much smaller than the colloidal particles used previously, which would result in much weaker electrostatic interactions even under conditions of equal charge density. This may explain why a considerably lower temperature relative to that at the cloud point is necessary to promote weak PDC attraction for BR. However, ammonium sulfate concentrations above 2.5 *M* were necessary to induce phase separation for $C_8\beta G_1$, at which point electrostatic repulsion is no longer significant. The polyoxyethylene surfactants used in the previous studies exhibit a cloud point temperature in binary mixtures, whereas for $C_8\beta G_1$ salt, PEG or other components are necessary for phase separation to occur. These results suggest that perhaps solute–solvent interactions are a significant barrier to promoting PDC crystallization. Kosmotropic salts such as ammonium sulfate or sodium malonate are strongly hydrated, thereby reducing the availability of water to the PDC (Cacace *et al.*, 1997). This is especially true at the high ionic strengths used in this study. Likewise, detailed crystallographic studies of proteins from halophilic archaebacteria also found a substantially higher degree of structural water associated with them than for their mesophilic counterparts (Dym *et al.*, 1995). This was attributed to a higher number of surface accessible charged amino acids, which led to an increase in stability at higher salt concentrations. Therefore, it is not unexpected that such high salt concentrations are necessary for crystallization of BR, nor when using $C_8\beta G_1$.

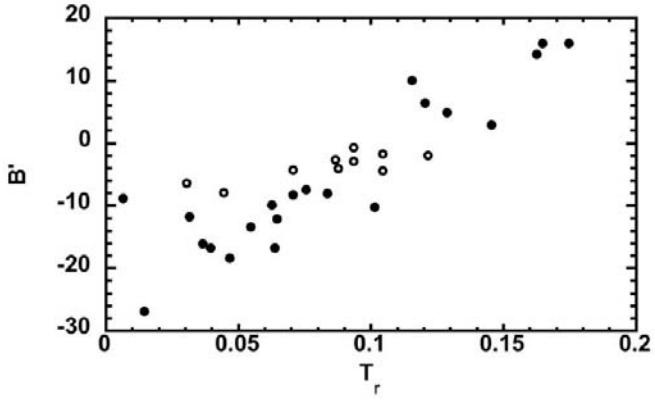

Figure 7
Comparison of PDC B_{22} values and $C_8\beta G_1$ cloud point temperatures at various solution conditions. Open circles denote conditions that led to crystal formation, with specific solution conditions for each given in Table 1.

5. Conclusions

Our results demonstrate for $C_8\beta G_1$-solubilized bacteriorhodopsin that the surfactant plays a key role in protein–detergent complex (PDC) interactions leading to crystallization. The value of this work lies in the much larger data set reported here than has been available previously, facilitated by use of self-interaction chromatography to measure PDC interactions, as well as elucidation of mechanisms that determine PDC interaction. In particular, we have shown the dual role of the surfactant in enhancing PDC attraction near the cloud point temperature as well as indirect action through excluded volume effects on PDC interactions. The latter may be important in preventing PDC interactions and in reducing the range of precipitant concentrations conducive to weak attraction. Minimizing this effect can be accomplished by reducing surfactant concentration to near CMC values. Overall, a detailed understanding of the variables controlling PDC interactions, as well as the availability of methods to characterize them and other solution properties, is a promising approach to the rational crystallization of membrane proteins.

This publication was made possible by NIH grant P20 RR-15588 from the COBRE Program of the National Center for Research Resources and NASA grant NAG8-1830 from the Microgravity Research Program. BWB gratefully acknowledges support through a NIH Chemistry–Biology Interface Training Grant T32 GM-08550 and NSF IGERT Graduate Fellowship DGE-0221651. We are grateful to George Turner of Seton Hall University for providing *H. halobium* strain ET1001 and to Gabriella Santonicola for assistance with dynamic light-scattering and surface-tension measurements.

References

Balzer, D. (1996). *Tenside Surfact. Det.* **33**, 102–111.
Blankschtein, D., Thurston, G. M. & Benedek, G. B. (1986). *J. Chem. Phys.* **85**, 7268–7288.
Cacace, M. G., Landau, E. M. & Ramsden, J. J. (1997). *Q. Rev. Biophys.* **30**, 241–277.
Connolly, M. L. (1983). *J. Appl. Cryst.* **16**, 548–558.

DasSarma, S. & Fleischmann, E. M. (1995). *Archaea-Halophiles: A Laboratory Manual.* New York: Cold Spring Harbor Laboratory Press.
Dencher, N. A. & Heyn, M. P. (1978). *FEBS Lett.* **96**, 322–326.
DePhillips, P. & Lenhoff, A. M. (2000). *J. Chromatogr. A*, **883**, 39–54.
Dym, O., Mevarech, M. & Sussman, J. L. (1995). *Science*, **267**, 1344–1346.
Garavito, R. M., Markovic Housley, Z. & Jenkins, J. A. (1986). *J. Cryst. Growth*, **76**, 701–709.
Garavito, R. M., Picot, D. & Loll, P. J. (1996). *J. Bioenerg. Biomembr.* **28**, 13–27.
Garavito, R. M. & Rosenbusch, J. P. (1986). *Methods Enzymol.* **125**, 309–328.
George, A. & Wilson, W. W. (1994). *Acta Cryst.* D**50**, 361–365.
Gottschalk, M., Dencher, N. A. & Halle, B. (2001). *J. Mol. Biol.* **311**, 605–621.
Guiochon, G., Golshan-Shirazi, S. & Katti, A. M. (1994). Editors. *Fundamentals of Preparative and Nonlinear Chromatography*. New York: Academic Press.
Heijne, G. von (1994). *Annu. Rev. Biophys. Biomol. Struct.* **23**, 167–192.
Hitscherich, C., Kaplan, J., Allaman, M., Wiencek, J. & Loll, P. J. (2000). *Protein Sci.* **9**, 1559–1566.
Hunte, C. (2002). In *Membrane Protein Purification and Crystallization: A Practical Guide*, edited by C. Hunte, G. von Jagow & H. Schagger, 2nd ed.. New York: Academic Press.
Koehler, R. D. & Kaler, E. W. (1997). *Langmuir*, **13**, 2463–2470.
Landau, E. M. & Rosenbusch, J. P. (1996). *Proc. Natl Acad. Sci. USA*, **93**, 14532–14535.
Laughlin, R. G. (1994). *The Aqueous Phase Behavior of Surfactants.* New York: Academic Press.
Liu, C. L., Nikas, Y. J. & Blankschtein, D. (1996). *Biotechnol. Bioeng.* **52**, 185–192.
Loll, P. J., Allaman, M. & Wiencek, J. (2001). *J. Cryst. Growth*, **232**, 432–438.
Loll, P. J., Hitscherich, C., Aseyev, V., Allaman, M. & Wiencek, J. (2002). *Cryst. Growth Des.* **2**, 533–539.
Lorber, B., DeLucas, L. J. & Bishop, J. B. (1991). *J. Cryst. Growth*, **110**, 103–113.
Luecke, H., Schobert, B., Richter, H. T., Cartailler, J. P. & Lanyi, J. K. (1999). *J. Mol. Biol.* **291**, 899–911.
McPherson, A. (2001). *Protein Sci.* **10**, 418–422.
McQuarrie, D. A. (2000). *Statistical Mechanics.* Sausalito, CA, USA: University Science Books.
Miercke, L. J. W., Ross, P. E., Stroud, R. M. & Dratz, E. A. (1988). *Biophys. J.* **53**, A377.
Miercke, L. J. W., Ross, P. E., Stroud, R. M. & Dratz, E. A. (1989). *J. Biol. Chem.* **264**, 7531–7535.
Patro, S. Y. & Przybycien, T. M. (1996). *Biotechnol. Bioeng.* **52**, 193–203.
Sato, H., Takeda, K., Tani, K., Hino, T., Okada, T., Nakasako, M., Kamiya, N. & Kouyama, T. (1999). *Acta Cryst.* D**55**, 1251–1256.
Schertler, G. F. X., Bartunik, H. D., Michel, H. & Oesterhelt, D. (1993). *J. Mol. Biol.* **234**, 156–164.
Schertler, G. F. X., Lozier, R., Michel, H. & Oesterhelt, D. (1991). *EMBO J.* **10**, 2353–2361.
Sehgal, D. & Vijay, I. K. (1994). *Anal. Biochem.* **218**, 87–91.
Shand, R. F. & Betlach, M. C. (1994). *J. Bacteriol.* **176**, 1655–1660.
Takeda, K., Sato, H., Hino, T., Kono, M., Fukuda, K., Sakurai, I., Okada, T. & Kouyama, T. (1998). *J. Mol. Biol.* **283**, 463–474.
Tessier, P. M., Johnson, H. R., Pazhianur, R., Berger, B. W., Prentice, J. L., Bahnson, B. J., Sandler, S. I. & Lenhoff A. M. (2003). *Proteins*, **50**, 303–311.
Tessier, P. M., Lenhoff, A. M. & Sandler, S. I. (2002). *Biophys. J.* **82**, 1620–1631.
Tessier, P. M., Vandrey, S. D., Berger, B.W., Pazhianur, R., Sandler, S. I. & Lenhoff, A. M. (2002). *Acta Cryst.* D**58**, 1531–1535.
Thiyagarajan, P. & Tiede, D. M. (1994). *J. Phys. Chem.* **98**, 10343–10351.
Zhang, R. T., Marone, P. A., Thiyagarajan, P. & Tiede, D. M. (1999). *Langmuir*, **15**, 7510–7519.